Acta Crystallographica Section F
Structural Biology and Crystallization Communications
ISSN 1744-3091

Crystallization and preliminary X-ray analysis of mouse RANK and its complex with RANKL

Thomas S. Walter,[a]‡ Changzhen Liu,[b]‡ Peng Huang,[c] Shiqian Zhang,[d] Lucy R. Wedderburn,[e] Bin Gao,[b,e] Raymond J. Owens,[a] David I. Stuart,[a] Peifu Tang[c]* and Jingshan Ren[a]*

[a]Division of Structural Biology and Oxford Protein Production Facility, The Wellcome Trust Centre for Human Genetics, The Henry Wellcome Building for Genomic Medicine, University of Oxford, Roosevelt Drive, Oxford OX3 7BN, England, [b]The Centre for Molecular Immunology, CAS Key Laboratory of Pathogenic Microbiology and Immunology (CASPMI), Institute of Microbiology, Chinese Academy of Sciences (CAS), 1 Beichen Xilu Road, Beijing 100101, People's Republic of China, [c]Department of Orthopaedics, Chinese PLA General Hospital, 28 Fuxing Road, Beijing 100853, People's Republic of China, [d]Department of Orthopaedics, The First Clinical College of Harbin Medical University, 23 Youzheng Street, Harbin 150001, People's Republic of China, and [e]Rheumatology Unit, UCL Institute of Child Health, London WC1N 1EH, England

‡ These authors contributed equally.

Correspondence e-mail: pftang301@126.com, ren@strubi.ox.ac.uk

Received 17 March 2009
Accepted 27 April 2009

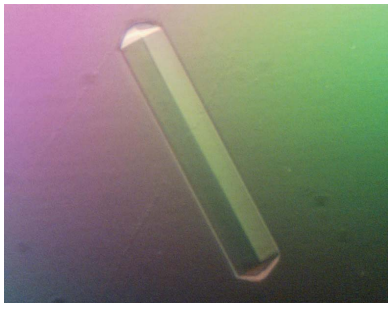

The interaction between the TNF-family molecule receptor activator of NF-κB ligand (RANKL) and its receptor RANK induces osteoclast formation, activation and survival in the process of bone remodelling. RANKL–RANK also plays critical roles in T-cell/dendritic cell communication and lymph-node formation and in a variety of pathologic conditions such as tumour-cell migration and bone metastasis. Both the ectodomain of mouse RANKL and the extracellular domain of mouse RANK have been cloned, expressed and purified. Crystals of RANK alone and of RANK in complex with RANKL have been obtained that are suitable for structure determination.

1. Introduction

The cytokines that belong to the tumour necrosis factor superfamily (TNFSF) and their associated receptor proteins (TNFRSFs) play critical roles in the control of cell differentiation and proliferation (Aggarwal, 2003). These large families have been extensively studied in the context of immunity and the coupling of lymphoid cells with other organ systems.

Bone remodelling is a dynamically balanced biological process involving bone-matrix synthesis by osteoblasts and bone resorption by osteoclasts. The interaction of TNFSF member 11 [receptor activator of nuclear factor κB ligand (RANKL), osteoclast differentiation factor (ODF) or TNF-related activation-induced cytokine (TRANCE)] and its receptor TNFRSF11A (RANK, TRANCE receptor) is essential for osteoclast formation from progenitor cells and the activation of mature osteoclasts and therefore plays a key role in the regulation of bone remodelling (Theill *et al.*, 2002; Walsh *et al.*, 2006). Osteoprotegerin (OPG, TNFRSF11B), a decoy receptor, is secreted primarily by bone-marrow stromal cells and osteoblasts (Simonet *et al.*, 1997). It acts as a soluble factor blocking the binding of RANKL to RANK; thus, RANKL, RANK and OPG provide a ligand/receptor/antagonist system, dysfunction in which can result in osteoporosis, arthritis or osteopetrosis. Activated T cells also express RANKL, while dendritic cells express RANK and provide a coupling of the immune system to bone-remodelling processes. Additionally, the RANK–RANKL interaction appears to be essential for the development of lymph organs. Intriguingly, this signalling mechanism has also been shown to be modulated by the female sex hormones progesterone and oestrogen and is key to the development of lactating mammary glands in pregnancy, thus providing a link to the high incidence of osteoporosis in women (Theill *et al.*, 2002; Walsh *et al.*, 2006).

RANKL, a type II transmembrane protein and the only known ligand of RANK, has been observed to occur in both a soluble form that arises from either proteolytic processing or alternative mRNA splicing and a membrane-spanning form. Both forms of RANKL are assembled into functional homotrimers like other members of the TNFSF (Dougall & Chaisson, 2006). RANK is a type I transmembrane protein containing an extracellular region consisting of four cysteine-rich domains (CRDs) and a large intracellular region of 383 residues. Receptor trimerization occurs upon interaction with RANKL, stimulating the recruitment of TNF-receptor-associated

factors (TRAFs) by the C-terminal cytoplasmic domain, with consequent stimulation of the AKT, JNK, ERK, p38, NFATc1 and NF-κB signalling pathways (Boyle *et al.*, 2003; Chung *et al.*, 2002; Feng, 2005; Takayanagi *et al.*, 2002).

To date, the three-dimensional structures of several ligands and receptors belonging to the TNFSF or TNFRSFs have been determined, including TNFα (Jones *et al.*, 1989), CD40L (Karpusas *et al.*, 1995), TNFRSF1A (Naismith *et al.*, 1996) and the poxvirus decoy receptor CrmE (Graham *et al.*, 2007). The structures of several ligand–receptor complexes, including the TNFβ–TNFRSF1A complex (Banner *et al.*, 1993) and the TRAIL–DR5 complex (Hymowitz *et al.*, 1999; Mongkolsapaya *et al.*, 1999), have also been resolved. The structure of mouse RANKL has been determined by three groups and shows an overall fold characteristic of the TNFSF (Ito *et al.*, 2002; Lam *et al.*, 2001; PDB code 1s55). However, to date the structure of RANK or of a complex with RANKL has not been determined. Since there is little sequence homology among the members of the TNFRSF other than disulfide-bonded cysteines and a few residues that are critical for the folding of the CRDs, it is not possible to build accurate models by modelling.

Here, we describe the expression, purification, crystallization and initial diffraction analysis of the functional extracellular domain of murine RANK (Swiss-Prot ID O35305, residues 26–210, molecular weight 20.3 kDa) and also of its complex with RANKL (Swiss-Prot ID O35235, residues 159–316, molecular weight 17.6 kDa). The structures of RANK and the RANKL–RANK complex will not only aid in understanding the functioning of the complex but will also shed more light on the specificity of the interactions among the TNF-like ligand–receptor complexes.

2. Material and methods

2.1. Protein cloning, expression and purification

A PCR product amplified from cDNA encoding the extracellular domain of murine RANK (residues 26–210) was cloned into the expression vector pET28a (Novagen; previously cut with the restriction enzymes *Nde*I and *Xho*I). The pET28a vector was used to express soluble RANK with two 6×His tags, one at each terminus (MGSSHHHHHHSSGLVPRGSHMHM and LEHHHHHH). The expression plasmid for GST-RANKL (residues 159–316), pGEX-6-RANKL, was a gift from Professor Fremont (Washington University School of Medicine, USA). Both recombinant proteins were expressed in *Escherichia coli* strain BL21-Gold (DE3). Bacteria with pET28-RANK were cultured in 2 l LB medium containing 100 µg ml^{-1} kanamycin at 310 K with agitation (250 rev min^{-1}) until an OD_{600} of 0.6 was attained. Isopropyl β-D-1-thiogalactopyranoside (IPTG, Sigma) was added to a final concentration of 1 m*M* for an additional 5 h to induce the expression of RANK. Bacteria with pGEX-6-RANKL were grown in a similar fashion, substituting 100 µg ml^{-1} ampicillin for kanamycin and using 0.2 m*M* IPTG for the induction of the expression of GST-RANKL over 12 h.

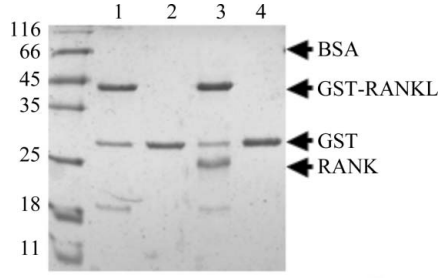

Figure 1
GST pull-down experiment showing that the recombinant RANK could associate with RANKL. Lane 1, GST-RANKL mixed with BSA; lane 2, GST mixed with BSA; lane 3, GST-RANKL with RANK; lane 4, GST with RANK. Molecular weights are indicated on the left in kDa.

The recombinant RANK was initially produced in the form of inclusion bodies. Bacteria expressing recombinant RANK were harvested by centrifugation and the pellet was resuspended in 100 ml ice-cold washing buffer (50 m*M* Tris, 150 m*M* NaCl, 5 m*M* EDTA, 1% Triton X-100, pH 8.0). The cells were disrupted and homogenized by sonication for 10 min (3 s on, 5 s off) using an Ultrasonic Cell Crusher (Scientz Biotech, Ningbo, China) and washed extensively with washing buffer. After repeated sonication and centrifugation, the inclusion bodies were dissolved at room temperature in 6 *M* guanidine hydrochloride (Gua-HCl), 50 m*M* Tris pH 8.5, 1 m*M* EDTA, 150 m*M* NaCl and 10 m*M* DTT to produce a final protein concentration of ∼30 mg ml^{-1}. The refolding of recombinant RANK was performed by further dilution with 20 m*M* Na_2HPO_4 pH 7.3, 1 *M* L-arginine, 20% glycerol, 10 m*M* reduced glutathione and 1 m*M* oxidized glutathione to a concentration of 10 mg ml^{-1}, followed by dialysis against 20 m*M* Na_2HPO_4 pH 7.3, 0.5 *M* L-arginine and 10% glycerol for 12 h at 277 K. Additional dialysis against 20 m*M* Na_2HPO_4 pH 7.3, 0.2 *M* L-arginine and 5% glycerol for 12 h at 277 K was followed by two dialysis steps against 20 m*M* Na_2HPO_4 pH 7.3 for 12 h at 277 K. After centrifugation at 20 000*g* for 10 min, the supernatant was purified by size-exclusion chromatography (SEC; Superdex 200, GE Healthcare) in 0.1 *M* Tris pH 7.0 and 50 m*M* NaCl.

The soluble extracellular domain of mouse RANKL was expressed as a glutathione *S*-transferase (GST) fusion protein. The fusion protein was purified by affinity chromatography with Glutathione-Sepharose Fast Flow 4B beads according to the manufacturer's instructions (GE Healthcare). Following cleavage of the tag with PreScission protease (PSP, GE Healthcare) overnight at 277 K, the RANKL was further purified by SEC (Superdex 200) in 0.1 *M* Tris pH 7.0 and 50 m*M* NaCl.

2.2. GST pull-down experiment

To demonstrate that the recombinant RANK and RANKL proteins possess correct folding and binding ability for each other, a pull-down experiment was performed. Cells expressing GST-RANKL and GST were lysed by sonication and the supernatants after centrifugation were incubated with Glutathione-Sepharose Fast Flow 4B beads for 2 h with gentle mixing at 277 K. Following extensive washing of the beads with 20 m*M* ice-cold PBS pH 7.3, soluble RANK (2 ml at 0.5 mg ml^{-1} in PBS) was added and mixed for 20 min. After washing, the bound proteins were eluted with 20 m*M* reduced glutathione in 50 m*M* Tris–HCl pH 8.0. Samples were subjected to SDS–PAGE and stained with Coomassie Blue R-250. As shown in Fig. 1, RANK bound to the immobilized GST-RANKL and migrated as a band of approximately 25 kDa (lane 3). In the control, no RANK was observed when RANK was incubated with GST alone (lane 4). The results clearly demonstrated that the recombinant proteins could associate specifically with each other, thus implying that both proteins were correctly folded.

2.3. Crystallization and data collection

Purified RANKL and RANK were concentrated to 10 mg ml^{-1} in solution buffered with 0.1 *M* Tris pH 7.0. Crystallization screening and optimization experiments for RANK and the RANKL–RANK complex were performed at 294 K using the sitting-drop vapour-diffusion method (100 nl + 100 nl mother liquor) in the crystallization

facility of the Oxford Protein Production Facility (Walter *et al.*, 2005; Mayo *et al.*, 2005).

Crystals of RANK were initially obtained in two conditions: (1) 20%(*w*/*v*) PEG 3350 and 0.2 *M* disodium tartrate and (2) 30%(*w*/*v*) PEG 5000 monoethyl ether (MME), 0.2 *M* ammonium sulfate and 0.1 *M* MES pH 6.5. Crystals grown in condition (1) were difficult to reproduce, whereas crystals grown in condition (2) were readily obtained but were usually observed to be multiple. By mixing the two crystallization solutions together, good-quality crystals could be obtained in crystallization drops containing 100 nl protein solution and 100 nl reservoir solution consisting of 10%(*w*/*v*) PEG 3350, 15%(*w*/*v*) PEG 5000 MME, 0.1 *M* ammonium sulfate, 0.1 *M* disodium tartrate and 0.05 *M* MES pH 6.5 (Fig. 2).

The protein solution for the RANKL–RANK complex was prepared by mixing the two proteins in a 1:1 molar ratio. Initial crystallization screens yielded nine crystal hits, all but one of which contained PEG 3350 and low concentrations of inorganic salts, including ammonium acetate, ammonium formate and sodium nitrate. The best crystals of the complex were grown from two optimized conditions: (1) 0.1 *M* sodium dihydrogen phosphate, 2 *M* sodium chloride, 0.1 *M* potassium dihydrogen phosphate, 0.1 *M* MES pH 6.5 and (2) 20%(*w*/*v*) PEG 3350 and 0.2 *M* ammonium formate. The crystallization drops contained 100 nl protein solution and 100 nl reservoir solution. Crystals grown in both conditions had the same morphology: long rods with a hexagonal cross-section. These crystals appeared within a week and took up to two months to reach maximum dimensions of 50 × 50 × 280 µm (Fig. 3).

X-ray diffraction data for RANK were collected on beamline BM14 at ESRF (Grenoble, France). A total of 180 images of 1.0° oscillation were collected from a single crystal of RANK at a wavelength of 0.954 Å. X-ray data for the RANKL–RANK complex were collected from a crystal grown in condition (1) on beamline ID23-EH2 of ESRF. 180 images of 1.0° oscillation were collected from two positions of a single crystal at a wavelength of 0.873 Å. A data set of 180° was also collected from a crystal of the complex grown in condition (2) on beamline I03 of Diamond at a wavelength of 1.060 Å. Crystals of the RANKL–RANK complex grown in condition (1) diffracted to higher resolution than those grown in condition (2). For crystals of both RANK and the complex, a cryoprotectant was prepared by adding glycerol to the mother liquor to a final concentration of 25%(*v*/*v*). This was then added to the crystallization drops. The crystals were cooled and maintained at 100 K under a cryostream of nitrogen gas during data collection. Data images were indexed, integrated and merged using *HKL*-2000 (Otwinowski & Minor, 1997). Table 1 shows the statistics of the X-ray data.

3. Results and discussion

The space group of the RANK crystals was $P2_12_12_1$, with unit-cell parameters a = 39.8, b = 94.3, c = 102.4 Å. The molecular weight of RANK, including the two His_6 tags, is 23.5 kDa. Assuming the presence of one or two molecules in the crystal asymmetric unit, the solvent content of the crystals was 69 or 39%, respectively. Judging from the strength of diffraction, it is likely that there are two molecules in the asymmetric unit. The self-rotation function showed a weak twofold noncrystallographic symmetry peak about 2σ above the background, indicating conformational differences between the two molecules in the asymmetric unit, which is in line with the RANK molecule having a thin elongated fold with great flexibility between

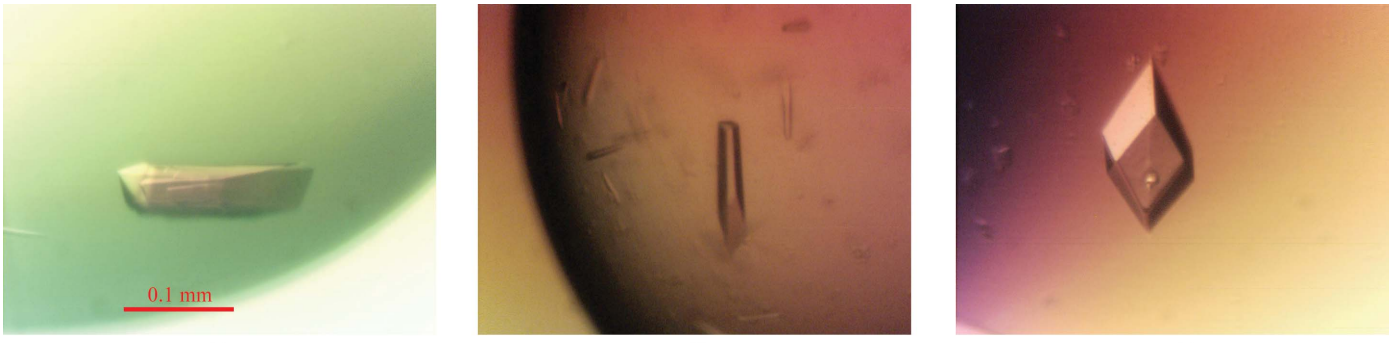

(*a*) (*b*) (*c*)

Figure 2
Crystals of RANK. The crystals in (*a*) and (*b*) were grown from conditions (1) and (2) of the initial crystallization screen, respectively. (*c*) shows a crystal obtained from the optimized condition.

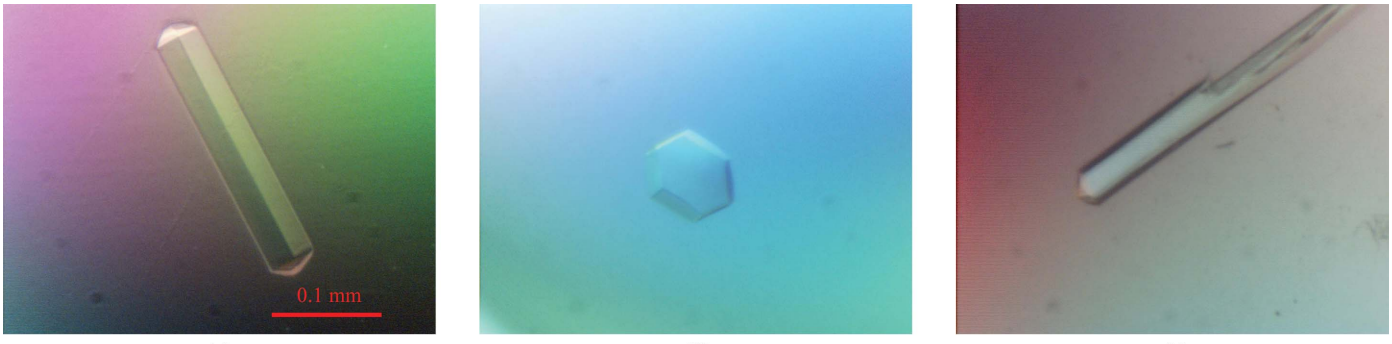

(*a*) (*b*) (*c*)

Figure 3
Crystals of the RANKL–RANK complex. (*a*) and (*b*) show crystals grown from condition (1). (*c*) shows a crystal grown from condition (2).

Table 1
X-ray data statistics.

Values in parentheses are for the highest resolution shell.

	RANK	RANKL–RANK (condition 1)	RANKL–RANK (condition 2)
X-ray source	BM14, ESRF	ID23-2, ESRF	I03, Diamond
Wavelength (Å)	0.9537	0.8726	1.0600
Space group	$P2_12_12_1$	$P6_3$	$P6_3$
Unit-cell parameters (Å)	a = 39.8, b = 94.3, c = 102.4	$a = b$ = 121.9, c = 94.5	$a = b$ = 122.4, c = 94.2
Resolution range (Å)	30.0–2.00 (2.07–2.00)	30.0–2.80 (2.90–2.80)	30.0–3.00 (3.11–3.00)
Unique reflections	26472 (2582)	19752 (1969)	15931 (1587)
Completeness (%)	99.6 (99.2)	100 (99.9)	99.9 (99.9)
Redundancy	6.9 (6.7)	8.8 (7.4)	9.8 (8.5)
Average $I/\sigma(I)$	17.7 (2.3)	11.2 (2.1)	10.5 (2.5)
$R_{\rm merge}$†	0.096 (0.644)	0.169 (0.820)	0.194 (0.725)

† $R_{\rm merge} = \sum_{hkl}\sum_i |I_i(hkl) - \langle I(hkl)\rangle| / \sum_{hkl}\sum_i I_i(hkl)$, where $I_i(hkl)$ is the observed intensity and $\langle I(hkl)\rangle$ is the mean intensity of i observations.

the four CRDs, as observed in structures of other multi-domain TNF-family receptors (Graham *et al.*, 2007; Naismith *et al.*, 1996).

Despite being grown in two different conditions, the RANKL–RANK complex crystals have the same hexagonal space group $P6_3$ and similar unit-cell parameters $a = b = 121.9$, $c = 94.5$ Å. The molecular weight of a heterohexameric RANKL–RANK complex, 127.5 kDa, is too large to be placed in the crystal asymmetric unit. As a heterohexameric form of the complex is expected, it is likely that the crystal asymmetric unit contains one third of the complex arranged with the threefold axis of the complex overlapping the threefold crystallographic symmetry. The calculated solvent content is 74%, which is consistent with the weak diffraction of these crystals. Structural solution and refinement of both structures is in progress.

The study was supported by the Beijing Municipal Natural Science Foundation (grant No. 30672135), the National Natural Science Foundation of China (grant No. 30700749), the CAS Talent Scheme, the UK Medical Research Council and the Biotechnology Biological Sciences Research Council. We thank the staff of beamline I03 at Diamond and of ID14-EH4 and ID23-EH2 at ESRF, Grenoble for help with data collections.

References

Aggarwal, B. B. (2003). *Nature Rev. Immunol.* **3**, 745–756.
Banner, D. W., D'Arcy, A., Janes, W., Gentz, R., Schoenfeld, H. J., Broger, C., Loetscher, H. & Lesslauer, W. (1993). *Cell*, **73**, 431–445.
Boyle, W. J., Simonet, W. S. & Lacey, D. L. (2003). *Nature (London)*, **423**, 337–342.
Chung, J. Y., Park, Y. C., Ye, H. & Wu, H. (2002). *J. Cell Sci.* **115**, 679–688.
Dougall, W. C. & Chaisson, M. (2006). *Cancer Metastasis Rev.* **25**, 541–549.
Feng, X. (2005). *Gene*, **350**, 1–13.
Graham, S. C., Bahar, M. W., Abrescia, N. G., Smith, G. L., Stuart, D. I. & Grimes, J. M. (2007). *J. Mol. Biol.* **372**, 660–671.
Hymowitz, S. G., Christinger, H. W., Fuh, G., Ultsch, M., O'Connell, M., Kelley, R. F., Ashkenazi, A. & de Vos, A. M. (1999). *Mol. Cell*, **4**, 563–571.
Ito, S., Wakabayashi, K., Ubukata, O., Hayashi, S., Okada, F. & Hata, T. (2002). *J. Biol. Chem.* **277**, 6631–6636.
Jones, E. Y., Stuart, D. I. & Walker, N. P. (1989). *Nature (London)*, **338**, 225–228.
Karpusas, M., Hsu, Y. M., Wang, J. H., Thompson, J., Lederman, S., Chess, L. & Thomas, D. (1995). *Structure*, **3**, 1031–1039.
Lam, J., Nelson, C. A., Ross, F. P., Teitelbaum, S. L. & Fremont, D. H. (2001). *J. Clin. Invest.* **108**, 971–979.
Mayo, C. J., Diprose, J. M., Walter, T. S., Berry, I. M., Wilson, J., Owens, R. J., Jones, E. Y., Harlos, K., Stuart, D. I. & Esnouf, R. M. (2005). *Structure*, **13**, 175–182.
Mongkolsapaya, J., Grimes, J. M., Chen, N., Xu, X. N., Stuart, D. I., Jones, E. Y. & Screaton, G. R. (1999). *Nature Struct. Biol.* **6**, 1048–1053.
Naismith, J. H., Devine, T. Q., Kohno, T. & Sprang, S. R. (1996). *Structure*, **4**, 1251–1262.
Otwinowski, Z. & Minor, W. (1997). *Methods Enzymol.* **276**, 307–326.
Simonet, W. S. *et al.* (1997). *Cell*, **89**, 309–319.
Takayanagi, H., Kim, S., Matsuo, K., Suzuki, H., Suzuki, T., Sato, K., Yokochi, T., Oda, H., Nakamura, K., Ida, N., Wagner, E. F. & Taniguchi, T. (2002). *Nature (London)*, **416**, 744–749.
Theill, L. E., Boyle, W. J. & Penninger, J. M. (2002). *Annu. Rev. Immunol.* **20**, 795–823.
Walsh, M. C., Kim, N., Kadono, Y., Rho, J., Lee, S. Y., Lorenzo, J. & Choi, Y. (2006). *Annu. Rev. Immunol.* **24**, 33–63.
Walter, T. S. *et al.* (2005). *Acta Cryst.* D**61**, 651–657.